



## Research Article

# JOURNAL OF APPLIED PHARMACEUTICAL RESEARCH | JOAPR

[www.japtronline.com](http://www.japtronline.com)

ISSN: 2348 – 0335

## FORMULATION AND EVALUATION OF PIPERACILLIN TAZOBACTAM LOADED AQUASOMAL GEL FOR THE TREATMENT OF NOMA

Sandeep S K, Anasuya Patil\*, Shafura S, Deepa Bagur Paramesh, Mahanthesh H M

### Article Information

Received: 14<sup>th</sup> January 2026

Revised: 2<sup>nd</sup> April 2026

Accepted: 3<sup>rd</sup> May 2026

Published: 15<sup>th</sup> May 2026

### Keywords

*Piperacillin, Tazobactam, Noma, Aquasomes, Central Composite Design*

### ABSTRACT

**Background:** Noma is a rapidly progressing gangrenous disease that affects the oral and facial tissues, mainly in malnourished and immunocompromised children. Delayed intervention often results in severe tissue destruction, facial deformity, and high morbidity. Although broad-spectrum antibiotics are routinely employed, conventional dosage forms often fail to achieve sufficient drug concentrations at the site of infection. Poor local absorption, limited tissue penetration, and the need for repeated administration reduce therapeutic effectiveness and patient compliance. Hence, a novel topical drug delivery system is required to enhance local drug delivery and clinical outcomes. This manuscript aims to formulate and evaluate a Piperacillin–Tazobactam-loaded Aquasomal gel for topical treatment of Noma. **Methodology:** Aquasomes composed of a calcium phosphate core coated with trehalose were prepared by the sonication method for topical delivery of Piperacillin–Tazobactam. A Central Composite Design (CCD) using Design-Expert® software was used to optimize formulation variables to improve entrapment efficiency and control drug release. The optimized Aquasomes were evaluated for particle size, polydispersity index, zeta potential, and drug entrapment efficiency, and then incorporated into a 1% Carbopol gel. **Results & Discussion:** The optimized formulation exhibited a particle size of 186 nm, a zeta potential of –19.37 mV, an entrapment efficiency of 68.18%, and sustained drug release of 61.1%. The gel exhibited suitable physicochemical properties and strong antibacterial activity against methicillin-resistant *Staphylococcus aureus*. **Conclusion:** The developed Aquasomal gel represents a promising topical therapy for the effective management of Noma.

### INTRODUCTION

Noma, also called cancrum oris, is a rapidly spreading gangrenous disease of the mouth and face, mainly affecting malnourished and immunocompromised children aged 2–6 years [1]. It begins as a gum ulcer and quickly destroys facial tissues, leading to severe abnormality and sometimes death if untreated [2]. Early signs include bleeding gums, foul breath,

and facial swelling. As it progresses, tissues die, exposing bones and teeth. Survivors often face difficulty eating, speaking, and social stigma [3]. Noma is most common in poor regions of Africa and Asia but can be prevented with good nutrition, hygiene, and timely antibiotic treatment [4]. Piperacillin and Tazobactam are broad-spectrum antibiotics belonging to BCS Class III, which means they have low permeability and poor oral

\*Department of Pharmaceutics, KLE College of Pharmacy, II Block, Rajajinagar, Bengaluru 560010, Karnataka, India

\*For Correspondence: [anasuya.raghu@gmail.com](mailto:anasuya.raghu@gmail.com)

©2026 The authors

This is an Open Access article distributed under the terms of the Creative Commons Attribution (CC BY NC), which permits unrestricted use, distribution, and reproduction in any medium, as long as the original authors and source are cited. No permission is required from the authors or the publishers. (<https://creativecommons.org/licenses/by-nc/4.0/>)

absorption because of first-pass metabolism. They are commonly used to treat severe gangrenous infections by blocking bacterial cell wall synthesis, leading to bacterial death [5]. However, their conventional intravenous (IV) form can be uncomfortable and less suitable for children, the elderly, or patients who have difficulty swallowing [6].

Calcium chloride and disodium hydrogen phosphate are key because they react to form a calcium phosphate core, which is biocompatible, biodegradable, and stable. This core helps protect sensitive drugs and allows controlled and sustained drug release in aquasomal gels [7]. Aquasomes play a key role in protecting sensitive drugs, such as proteins, enzymes, and genes, from damage while preserving their biological activity. They have a three-layer structure consisting of a core, a coating, and a drug layer, which together provide stability, biocompatibility, & controlled drug release [8].

The carbohydrate coating prevents structural changes, and the nanocrystalline core offers strength and slow degradation. This system enhances the solubility, bioavailability, and targeted delivery of poorly soluble drugs, resulting in improved therapeutic efficacy with fewer side effects [9]. Aquasome-based gels are designed to provide sustained drug release, improved patient comfort, and targeted action. These tiny spherical nanocarriers (60–300 nm) have a solid core, a protective sugar coating & a drug layer that helps the drug to reach the bloodstream effectively through noninvasive routes [10]. Overall, Aquasomes are considered one of the better and more effective formulations for delivering delicate and unstable drugs.

## MATERIAL AND METHODS

### Materials

Piperacillin sodium and Tazobactam were obtained from BLD Pharma, Hyderabad; Trehalose, Calcium Phosphate, Calcium chloride, Disodium hydrogen phosphate, Glycerine, Carbopol 934, and Triethanolamine were purchased from Yarrow Chemicals, Mumbai; while Propylene glycol was procured from SD Fine Chem Ltd., Mumbai.

### Methods

Aquasomes were prepared by sonication, using calcium phosphate as the core material, trehalose as the coating material, and piperacillin/tazobactam as the drug. Firstly, a ceramic core was prepared by using the co-precipitation technique. A 0.75 M

disodium hydrogen phosphate solution was slowly added to a 0.25 M calcium chloride solution, and the mixture was then sonicated for 2 hours to form the core. Then, the prepared ceramic core is coated with trehalose, and the mixture is sonicated for about 90 minutes to achieve a uniform coating. The coated particles are filtered, dried, and stored at 2°C.

Further, the trehalose-coated core was dispersed in a piperacillin-tazobactam solution, and the drug was dissolved in a pH 6.8 phosphate buffer. The dispersion was kept at 2°C overnight to ensure proper adsorption of the drug onto the surface. And finally, the formulation was freeze-dried to obtain piperacillin-tazobactam-loaded aquasomes [11].

### Optimization using Central composite design

A Central Composite Design was applied using Design-Expert® software (version 13.0.5.0) to optimize the formulation of piperacillin–tazobactam Aquasomes. Trehalose and calcium phosphate were selected as key formulation factors, and their effects on entrapment efficiency (%) and in-vitro drug release (%) were studied. The batches were prepared as per the randomized runs generated by the design in Table 1 (A, B) [12].

## CHARACTERIZATION OF PTZ AQUASOMES

### Particle size distribution

The particle size and polydispersity index of the Aquasomes were measured using a Malvern Zeta sizer at 25°C. A 1 ml sample was transferred into a polystyrene cuvette and analyzed to determine its size distribution [13].

### Zeta potential

The zeta potential of the aquasomes was measured using a Malvern ZetaSizer at 25°C. A 1 mL sample was placed in a polystyrene cuvette, and a zeta dip cell was used to measure the zeta potential [14].

**Table 1 (A): List of dependent and independent variables**

Independent variables (Factors)		Dependent variables (Responses)
A	Calcium phosphate	<i>In vitro</i> drug release
B	Trehalose	Entrapment efficiency

Factor	Name	Units	Type	Min	Max
A	Calcium phosphate	gm	numeric	0.049999	5.00061
B	Trehalose	mg	numeric	8.49042	290.502

**Table 1(B): Formulation Chart of Aquasomal gel A:**

Formulation code	Factor 1: Calcium Phosphate (gm)	Factor 2: Trehalose (mg)
FPTZ 1	2.95	290.502
FPTZ 2	2.95	8.49042
FPTZ 3	2.95	149.496
FPTZ 4	0.89939	249.202
FPTZ 5	5.00061	249.202
FPTZ 6	2.95	149.496
FPTZ 7	2.45	197.684
FPTZ 8	2.95	149.496
FPTZ 9	2.95	149.496
FPTZ 10	5.85	149.496
FPTZ 11	0.89939	49.79
FPTZ 12	0.0499995	149.496
FPTZ 13	5.00061	49.79

**Entrapment efficiency**

For entrapment efficiency, 1 ml of the formulation was centrifuged at 10,000 rpm for 1 hour at 4°C. The supernatant was collected, and the amount of untrapped drug was measured using UV spectroscopy at 262 nm. Entrapment efficiency was calculated using the standard formula [15].

$$EE\% = \frac{\text{Amount of drug added} - \text{Amount of free drug in the supernatant}}{\text{Amount of drug added}} \times 100$$

**Preparation of PTZ-loaded aquasomal gel**

The piperacillin–tazobactam Aquasomes were incorporated into a 1% Carbopol 934 gel to prepare the final formulation. For the gel base, 1 g of Carbopol 934 is dissolved in 100 ml of distilled water, stirred for 2 hours, and left to swell overnight. The optimized Aquasomes (containing 50 mg of the drug) and 50 mg of pure drug were separately mixed into 10 g of the 1% Carbopol gel to obtain a 1% Aquasome gel. Triethanolamine was added with continuous stirring to adjust the gel consistency and achieve the desired buccal formulation [16,17].

**Measurement of pH**

About 1 g of the Aquasomal gel was weighed and diluted with 20 ml of distilled water. The mixture was then checked using a pH meter. The measurement was repeated three times, and the average pH value was recorded [18].

**Spreadability measurements**

Spreadability testing was performed to estimate the gel's viscosity and ease of spreading. For this test, 1 g of the Aquasomal gel was placed between two glass slides of equal thickness (25 inches). A 1 kg weight was placed on the top slide for 1 minute to allow the gel to spread. After removing the weight, the gel diameter (in cm) was measured [19].

**Drug content**

About 0.5 g of the gel was mixed with 10 ml of ethanol and then filtered. The filtrate was diluted with phosphate buffer to restore the volume. From this solution, 1 ml was taken and made up to 10 ml using phosphate buffer. The absorbance of the final solution was measured at 262 nm using a UV–visible spectrophotometer [20].

**Determination of viscosity**

The viscosity of the formulation was measured using a Brookfield viscometer with an SCA-18 spindle. The sample was kept at 25°C, and the spindle was fully immersed in it. As the spindle began to rotate, the resistance from the gel was transferred to the instrument's calibrated spring. The viscosity was then recorded based on the spring's deflection [21].

**FT-IR spectroscopy (FT-IR Analysis)**

Infrared spectrophotometry was done for the drug & excipients used in the formulation. A measured amount of the drug was mixed with potassium bromide (KBr) and finely ground, and the mixture was scanned in the 4000–400 cm<sup>-1</sup> range to obtain the FT-IR spectrum [22,14].

**Differential scanning calorimetry (DSC)**

DSC was carried out for the pure drug, the excipients, and their physical mixture using a DSC-60 Shimadzu instrument. Each sample was sealed in an aluminium pan and heated from 25°C to 300°C at a rate of 10°C/min under a nitrogen atmosphere. The resulting DSC curves were compared to check for any possible interactions between the drug and excipients [23].

**Scanning Electron Microscopy (SEM)**

The morphological characteristics of the Aquasomal formulation were analyzed using a High-Resolution Scanning Electron Microscope, where particle size, shape, and surface morphology were assessed for the optimized PTZ-loaded aquasome formulation [24].

### In vitro drug release

A drug release study is performed using a semipermeable membrane. One end of a test tube was covered with the membrane, and 1 ml of FPTZ 7 was added through the open end. The membrane side was then placed in a pH 6.8 buffer and stirred continuously throughout the experiment. At fixed time intervals, 5 ml samples were collected to measure the amount of drug released. These samples were analyzed at 262 nm using UV spectroscopy to determine the concentration of PTZ [25].

### Drug release kinetics study

Data obtained from zero-order, first-order, Higuchi, and Korsmeyer–Peppas models were used to study the drug-release behavior of the formulation. Graphical plots for each model were prepared and compared. The model with the highest R<sup>2</sup> value was considered the best to explain the formulation's release mechanism [26].

### Antibacterial activity of Aquasomal gel

The pathogenic strain, methicillin-resistant *Staphylococcus aureus*, was grown in Brain Heart Infusion (BHI) medium and incubated at 37°C for 24 hours to obtain an active culture [27].

### Well diffusion assay protocol

BHI agar (1.5% w/v) was mixed with 1% (v/v) of the bacterial culture and poured into sterile petri plates to solidify. Wells of 5 mm were made using a sterile cork borer, and 100 µl of each sample was added to the wells. The plates were kept at 4°C for 30 minutes to allow proper diffusion, then incubated at 37°C for 24–48 hours. The zone of inhibition (mm) was measured.

### Ex vivo permeation study

*Ex vivo* skin permeation study of the selected PTZ-loaded Aquasomal gel was carried out using goat buccal mucosa in a Franz diffusion cell. The mucosa was soaked in pH 6.8 phosphate buffer before use. It was then placed between the donor and receptor compartments of the cell. About 50 mg of the Aquasomal gel was applied to the mucosal surface in the donor compartment. The receptor compartment contained 7 ml of pH 6.8 buffer, with a magnetic stirrer rotating at 50 rpm, and was maintained at 37 ± 0.5°C. Samples were collected at regular intervals for 10 hours and replaced with fresh buffer to maintain sink conditions. The collected samples were analyzed at 262 nm using a UV spectrophotometer. The cumulative percentage permeation per unit area was calculated and plotted as a function of time [28].

## RESULTS AND DISCUSSION

Central Composite Design (CCD) was chosen for its ability to optimize formulations with both linear and nonlinear factor effects. The model permitted the assessment of main effects and quadratic effects on critical responses, such as entrapment efficiency and in vitro drug release, as shown in Table 2, where the in vitro drug release profile of FPTZ 1 to FPTZ 13 is illustrated in Figure 1 (E). CCD efficiently investigated the design space with fewer runs than a full factorial design while retaining model reliability. It enabled the precise prediction of optimal formulation conditions within a predefined range [29].

**Table 2: Response of in-vitro drug release, Entrapment efficiency**

Formulation code	Entrapment efficiency (%)	In-vitro drug release (%)
FPTZ1	76.2	54.3
FPTZ2	70.5	58.7
FPTZ3	67.3	60.2
FPTZ4	60.8	67.2
FPTZ5	78.4	50.1
FPTZ6	68.2	60.2
FPTZ7	68.1	61.1
FPTZ8	66.5	61.7
FPTZ9	69.3	59.9
FPTZ10	69	49.7
FPTZ11	61.5	66.5
FPTZ12	55.4	72.3
FPTZ13	69	50.5

### In-vitro Drug Release %

$$Y = 61.14 - 8.133A - 0.740B - 0.275AB + 0.356A^2 - 1.894B^2$$

The drug release data from the Aquasomal formulation was fitted to a quadratic model, and the final equation showed how calcium phosphate (A) and trehalose (B) affect the release rate. The model was highly reliable, as indicated by its large F-value (141.82) and very low p-value (p < 0.0001), confirming that the results were not due to random error.

Among all the factors, the amount of calcium phosphate and the quadratic effect of trehalose had the strongest impact on drug release (p < 0.05). The model also showed excellent accuracy and predictability, with high R<sup>2</sup> (0.9902), adjusted R<sup>2</sup> (0.9832), and predicted R<sup>2</sup> (0.9305), along with a low standard deviation and high adequate precision, indicating a strong signal-to-noise ratio (Table 3).

The contour & 3D surface plots showed that increasing calcium phosphate noticeably decreased drug release, possibly because it increased particle density & slowed matrix breakdown. Trehalose showed a curved (non-linear) effect, where both very low & very high levels reduced release, likely due to changes in surface stability and hydration, as shown in Figure 1 (A, B).

#### Entrapment efficiency (EE%)

$$Y = 68.13 + 8.309A + 1.095B + 0.525AB - 1.263A^2 + 1.813B^2$$

The Entrapment efficiency (EE%) model showed a very high F-value of 102.41, indicating that the model is statistically reliable and that the chance of the results occurring by random error is extremely low (0.01%). The factors that significantly affected EE% were calcium phosphate (A), trehalose (B), and their quadratic terms ( $A^2$  and  $B^2$ ), as their p-values were below 0.05. The positive coefficient for calcium phosphate (A) indicates that increasing its amount improves EE%. However, the negative quadratic term ( $A^2$ ) indicates that beyond a certain level, too much calcium phosphate can decrease EE%, possibly due to particle saturation or aggregation. Trehalose (B) showed a small positive linear effect, while its positive quadratic term ( $B^2$ ) suggests that higher concentrations further improve EE%. The interaction term (AB) was also positive, indicating that using both calcium phosphate and trehalose together improves entrapment efficiency, as shown in Figures 1(C) and 1 (D). The model fit was very strong, with high  $R^2$  (0.9865), adjusted  $R^2$  (0.9769), and predicted  $R^2$  (0.9041), indicating excellent accuracy and predictive ability, as shown in Table 3. The Adequate Precision value of 33.61, which is much higher than the required minimum of 4, confirms that the model has a strong signal and is suitable for navigating the design space.

#### OVERLAY PLOT OF OPTIMIZED FORMULATION

The formulation was optimized using a quadratic model, and an overlay plot was used to identify the ideal design space where both entrapment efficiency and *in vitro* drug release meet the desired targets. The polynomial equation showed that higher concentrations of calcium phosphate significantly reduced drug release, while Trehalose had a smaller negative effect. Interaction and quadratic terms indicated curvature in the response. The optimized point was  $\text{Ca}_3(\text{PO}_4)_2 = 2.4568$  g and Trehalose = 197.684 mg, yielding a predicted EE of 68.12% and a release of 61.41%, which closely matched the experimental values. This confirmed the model's accuracy and suitability, as shown in Figure 1 (F).

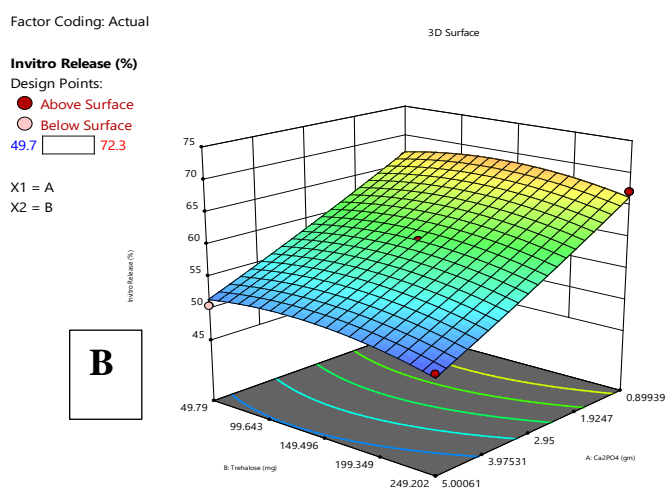
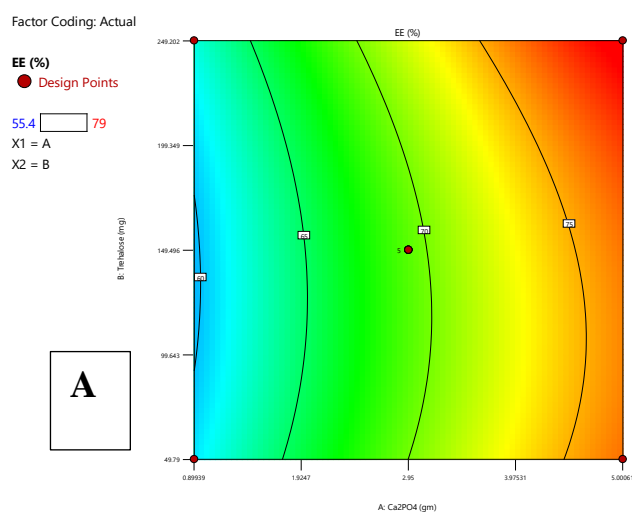
#### Selection of optimized formulation

Based on observed responses, formulation (F-PTZ 7) was selected, as it showed 61.41% *in vitro* drug release and 68.12% entrapment efficiency. Therefore, this formulation (F-PTZ 7) was further characterized and evaluated.

#### EVALUATION OF OPTIMIZED FORMULATION (F-PTZ 7)

##### Particle size, PDI, and Zeta potential

The (F-PTZ 7) Aquasomal system containing actively loaded piperacillin–tazobactam was assessed for its zeta potential, particle size, and PDI. The particles measured 186 nm, confirming their nanoscale nature. The zeta potential of  $-19.37$  mV suggested good electrostatic stability, which is beneficial for topical use, as it can improve skin permeation and support sustained drug release. The PDI was 0.3697, indicating a fairly uniform particle size distribution, and a value below 1.0 confirms good homogeneity and overall formulation consistency [13].



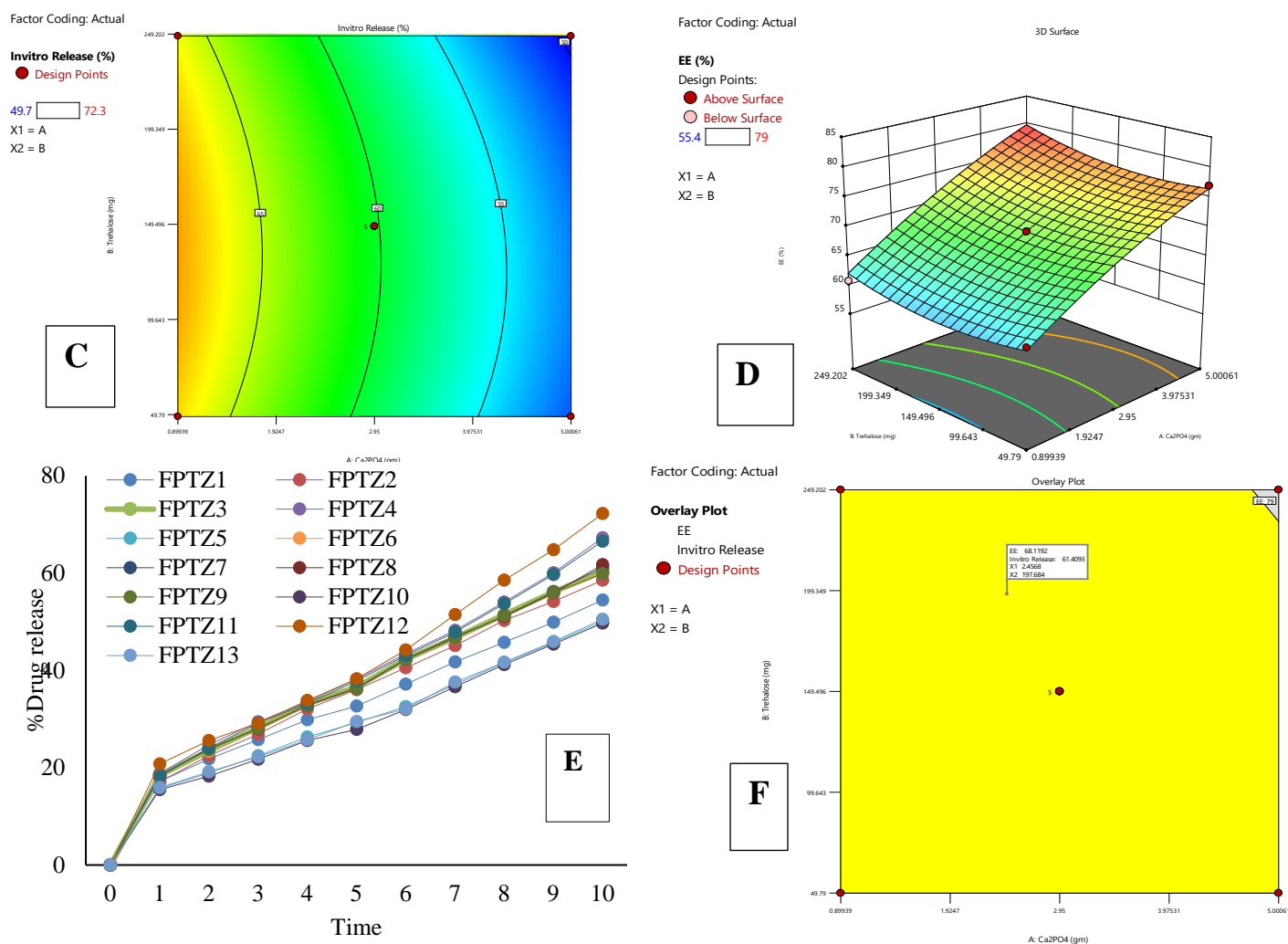


Figure 1: A is a contour plot, and B is a 3-D Surface plot of in vitro drug release. C is a contour plot, and D is a 3-D surface plot of Entrapment efficiency, E is in vitro dissolution of FPTZ 1-FPTZ 13, and F is an overlay plot of FPTZ 7.

Table 3: Results of regression analysis and polynomial coefficients relating to each critical parameter attribute (CPAS)

Response	F-value	p-value	R <sup>2</sup>	Adjusted R <sup>2</sup>
In vitro drug release	141.82	< 0.0001	0.9902	0.9832
Regression equation of the fitted model				
$Y = 61.14 - 8.133A - 0.740B - 0.275AB + 0.356A^2 - 1.894B^2,$				
Entrapment efficiency	102.41	< 0.0500	0.9865	0.9769
Regression equation of the fitted model				
$Y = 68.13 + 8.309A + 1.095B + 0.525AB - 1.263A^2 + 1.813B^2,$				

**FT-IR Analysis**

FT-IR analysis was performed on PTZ, trehalose, and their physical mixture to evaluate potential drug excipient

interactions, as presented in Figure 2(a). The FTIR spectra of the physical mixture exhibited all characteristic peaks of the pure drug with no significant disappearance of Functional group bands. This shows the absence of chemical interactions between piperacillin, tazobactam, and the selected excipients, confirming the compatibility for PTZ-loaded Aquasomal gel [30].

**Differential Scanning Calorimetry (DSC)**

Differential scanning calorimetry analysis was conducted for the pure drug, individual excipients, and their physical mixture. The thermogram of PTZ showed distinct endothermic peaks at 187.13°C and 195.87°C, corresponding to its melting point and confirming its crystalline nature. In contrast, the thermogram of the excipients, physical mixture, and drug showed shifted endothermic peaks with reduced intensity. These findings confirm the thermal compatibility of PTZ with selected excipients for Aquasomal gel, as illustrated in Figure 2(b) [31].

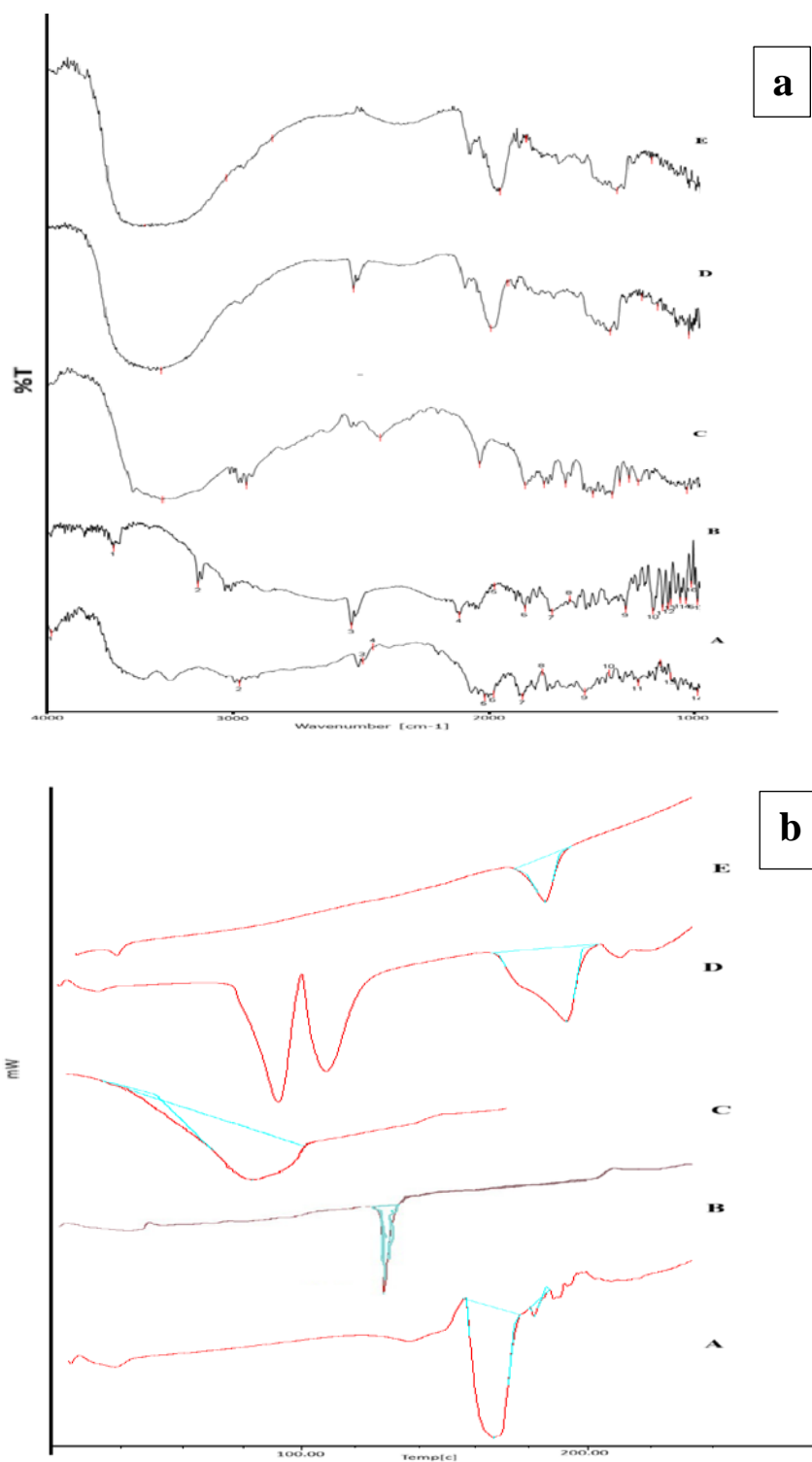


**Figure 2: a) FTIR, b) DSC of Drug excipient and formulation where A is piperacillin, B is Tazobactam, C is Trehalose, D is Physical mixture, E is FPTZ 7**

### Scanning Electron Microscopy

SEM analysis of the optimized FPTZ 7 Aquasomes revealed that the particles were evenly distributed, with sizes ranging from 66.5 to 140 nm (Figure 3). The SEM images indicate that the

drug was successfully bound to the Aquasomes. These features suggest that the formulation is suitable and promising for PTZ-loaded Aquasomes, indicating successful drug adsorption and effective topical use. In the particle size (DLS) analysis, the

hydrated state, including the surrounding hydration layer, was observed to yield larger sizes, whereas in SEM, it measures particles in the dry state, showing the actual physical size [25]

### EVALUATION OF FPTZ 7

**pH:** The pH of the Aquasomal formulations was found to be around  $6.8 \pm 0.05$ , which closely matches the natural pH of the human buccal mucosa. This indicates that the formulation is suitable for buccal application. The reported pH value represents the average of three measurements [32].

### Spreadability Measurements

The Aquasomal gel containing 1% Carbopol showed a spreadability of  $13.3 \pm 0.14$  cm. The presence of Carbopol helps the gel spread easily with minimal effort. This ensures smooth application, better contact with the skin, and reduces the chance of the gel running or leaking. Together, these features support improved therapeutic effectiveness [33].

### Drug Content

The drug content of the prepared Aquasomal gels ranged from **80.15% to 86.67%**, indicating that almost no drug was lost during gel preparation. This indicates that the method used to mix the drug into the gel was effective, helping keep the active ingredient stable and well-retained throughout the formulation process [34].

### Viscosity

The optimized gel containing 1% Carbopol showed a viscosity of 342.8 cPs. As the amount of Carbopol increases, the gel thickens because more cross-linking occurs in the formulation. Rheological studies showed that the gel exhibits shear-thinning behavior, meaning it becomes thinner when spread, allowing smooth application without running. Its thixotropic property also helped the gel spread easily and quickly return to its original consistency after use [35].

### In vitro Dissolution of Aquasome and FPTZ 7

Both the optimized Aquasomal formulation and FPTZ 7 were tested for in vitro drug release over 10 hours using the FDC method with a dialysis membrane. Samples were collected every hour to measure the amount of drug released. The results showed an improved release pattern, with a total drug release of **71.9%** as shown in Figure 4 (A). This controlled release over 10 hours indicates that the Aquasomal gel can hold the drug effectively and release it slowly, helping to maintain its action for a longer time [36,37].

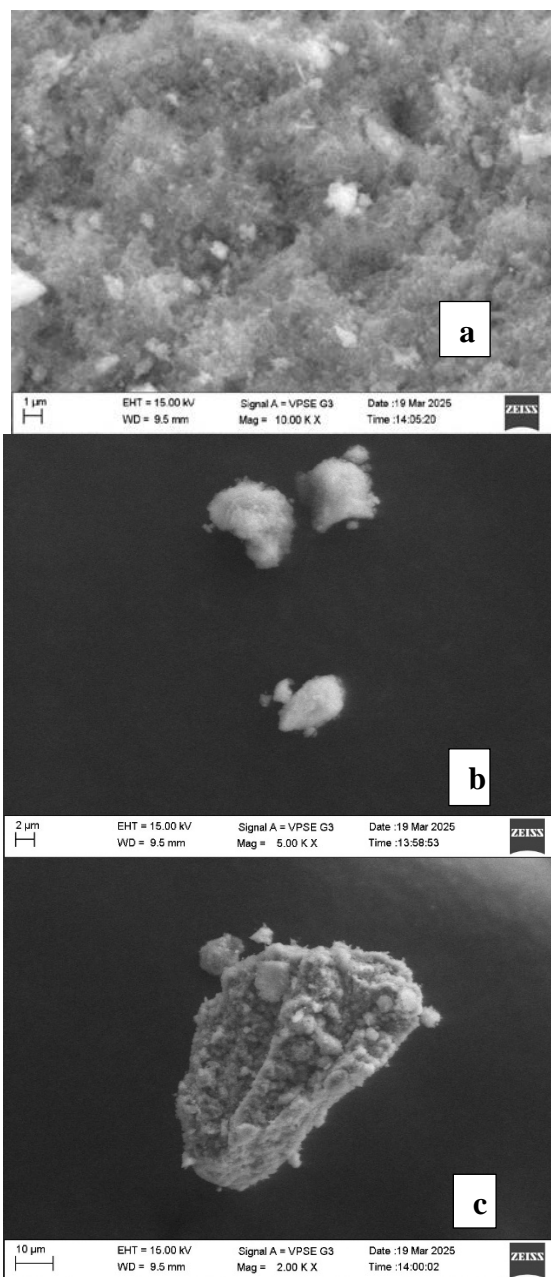


Figure 3 (a, b, c): SEM images of FPTZ 7 formulation

### Drug Release Kinetics

The in vitro drug release profile of the FPTZ 7 formulation was analyzed using various kinetic models: zero-order, First-order, Higuchi, and Korsmeyer–Peppas models. The release data demonstrated the best fit to the first-order model, as indicated by the highest correlation coefficient ( $R^2 = 0.9758$ ), confirming a diffusion-controlled release mechanism shown in Figure 4(B). Further evaluation using the Korsmeyer–Peppas model yielded an  $n$  value of 1.203, which corresponds to a non-Fickian (anomalous) transport mechanism, suggesting that drug release is governed by both diffusion and polymeric matrix relaxation processes [38,39].

**Ex vivo Permeation studies**

A Drug permeation study was conducted on goat mucosa, demonstrating that the PTZ gel effectively delivered the drug through the mucosa. The formulation achieved a cumulative drug permeation of 4.212308 mg/cm<sup>2</sup> over 10 hours, with a steady-state flux of 0.5363mg/cm<sup>2</sup>/h, as shown in Figure 4(C), and a permeability coefficient of 0.00421cm/h. The gel provided a slow and steady release of the drug, supported by its efficient gel structure. A notable improvement in drug permeation was observed, which is mainly due to the presence of trehalose. Trehalose acted as both a stabilizer and a permeation enhancer, helping the drug pass more effectively through the mucosa [40].

**Antibacterial activity**

The optimized FPTZ 7 gel exhibited strong antibacterial activity against methicillin-resistant *Staphylococcus aureus* as determined by the well-diffusion method (Figure 5). The gel produced a **28 mm** zone of inhibition, which was greater than that of the pure drug (**26 mm**) and the standard antibiotic (**18 mm**), as shown in Table 4. The blank sample showed no antibacterial effect. These findings show that the Aquasomal gel improved the drug’s effectiveness, likely due to better drug loading and improved penetration into the bacteria [41,42].

**Table 4: Zone of inhibition activity**

Sample	Zone of inhibition (mm in diameter) <i>S. aureus</i>
FM (Formulation)	28
PD (Pure drug)	26
Antibiotic (Std antibiotic)	18
BLK (Blank)	--

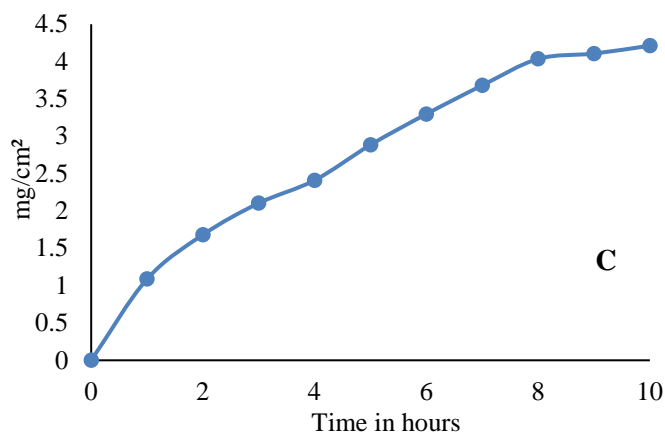
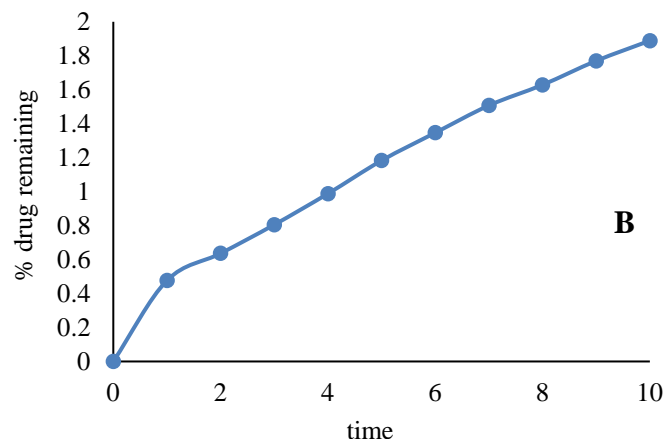
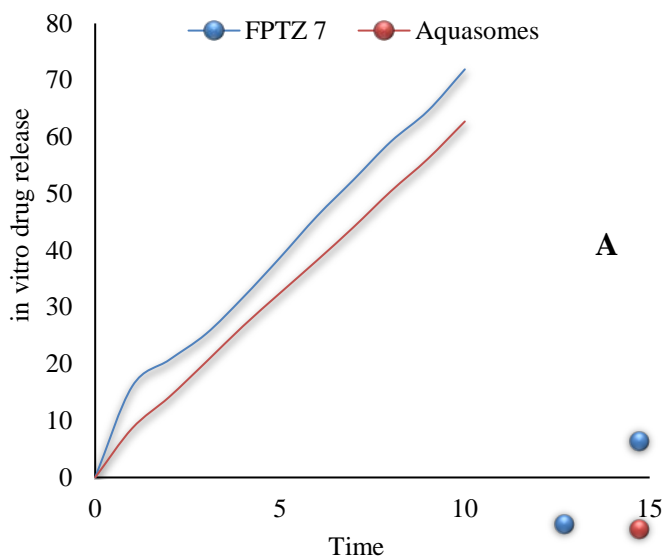


**Figure 4: A is the in vitro dissolution of Aquasome and FPTZ 7, B is first-order release kinetics, and C is an ex vivo permeation study of FPTZ 7.**

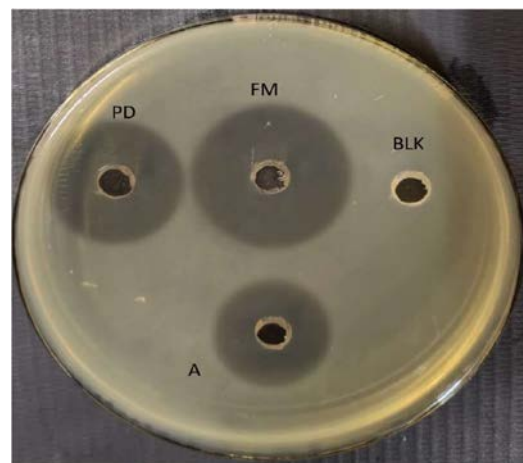


**Figure 5: Antibacterial activity of the given sample against methicillin-resistant *Staphylococcus aureus***

**Statistical analysis**

A Student’s t-test was performed to compare the Zone of Inhibition between the pure drug and the formulation. The obtained p-value was 0.0705, indicating that the increase is not statistically significant ( $p > 0.05$ ).

**CONCLUSION**

The present study mainly aimed to develop and evaluate a transdermal Aquasomal gel formulation of piperacillin-tazobactam for the effective treatment of Noma. The conventional routes have drawbacks, including low oral bioavailability, a short half-life, and poor patient compliance. To overcome these challenges, Aquasomes, three-layered nanocarriers with a calcium phosphate core and a trehalose coating, were created via sonication and optimized using Central Composite Design. The optimized formulation FPTZ 7 has a particle size of 186 nm, a zeta potential of -19.37 mV, and an Entrapment effectiveness of 68.18%. The Aquasomes were mixed into a 1% carbopol gel and tested in both *in vitro* and *ex vivo* studies. The gel released 71.9% of the drug during 10 hours, with a cumulative penetration of 4.212308 mg/cm<sup>2</sup>. Antibacterial investigations revealed a 28-mm zone of inhibition against methicillin-resistant *Staphylococcus aureus*, indicating its potential for localized and sustained drug delivery and confirming that the Aquasomal gel is a promising system for sustained, localized delivery of piperacillin-tazobactam in the treatment of NOMA.

**FINANCIAL ASSISTANCE**

NIL

**CONFLICT OF INTEREST**

The authors declare no conflict of interest.

**AUTHOR CONTRIBUTION**

Sandeep S K and Mahanthesh H M were involved in the investigation (bench experiments) and the preparation of the original draft. Anasuya Patil contributed to conceptualization, formal analysis, writing review, and editing. Shafura S carried out the literature review and assisted in writing. Deepa Bagur Paramesh supported the literature search and contributed to writing, reviewing, and editing.

**REFERENCES**

- [1] Marck KW. Cancrum oris and noma: some etymological and historical remarks. *Br J Plast Surg*, **56(6)**, 524–527 (2003) [https://doi.org/10.1016/S0007-1226\(03\)00224-8](https://doi.org/10.1016/S0007-1226(03)00224-8)
- [2] Maguire BJ, Shrestha P, Rashan S, Shrestha R, Harriss E, Varenne B, Guérin PJ. Protocol for a systematic review of the evidence-based knowledge on the distribution, associated risk factors, the prevention and treatment modalities for noma. *Wellcome Open Res*, **8**, 125 (2023) <https://doi.org/10.35802/222410>
- [3] Galli A, Brugger C, Fürst T, Monnier N, Winkler MS, Steinmann P. Prevalence, incidence, and reported global distribution of noma: a systematic literature review. *Lancet Infect Dis*, **22(8)**, e221–e230 (2022) [https://doi.org/10.1016/S1473-3099\(21\)00698-8](https://doi.org/10.1016/S1473-3099(21)00698-8)
- [4] Srouf ML, Marck K, Baratti-Mayer D. Noma: overview of a neglected disease and human rights violation. *Am J Trop Med Hyg*, **96(2)**, 268–274 (2017) <https://doi.org/10.4269/ajtmh.16-0718>
- [5] Lee YJ, Kang G, Zang DY, Lee DH. Population pharmacokinetic modeling of piperacillin/tazobactam in healthy adults and exploration of optimal dosing strategies. *Pharmaceuticals*, **18(8)**, 1124 (2025) <https://doi.org/10.3390/ph18081124>
- [6] Hayashi Y, Roberts JA, Paterson DL, Lipman J. Pharmacokinetic evaluation of piperacillin-tazobactam. *Expert Opin Drug Metab Toxicol*, **6(8)**, 1017–1031 (2010) <https://doi.org/10.1517/17425255.2010.506187>
- [7] Ayom GE, Malima NM, Owonubi SJ, Revaprasadu N. Aquasomes: a novel nanocarrier system for drug delivery. In: *Advanced Nanoformulations*. Academic Press, 289–309 (2023) <https://doi.org/10.1016/B978-0-323-85785-7.00018-8>
- [8] Umashankar MS, Sachdeva RK, Gulati M. Aquasomes: a promising carrier for peptides and protein delivery. *Nanomedicine*, **6(3)**, 419–426 (2010) <https://doi.org/10.1016/j.nano.2009.11.002>
- [9] Banerjee S, Sen KK. Aquasomes: a novel nanoparticulate drug carrier. *J Drug Deliv Sci Technol*, **43**, 446–452 (2018) <https://doi.org/10.1016/j.jddst.2017.11.011>
- [10] Sahu V, Sahoo SK, Sahoo AC. Aquasome: as drug delivery carrier in the pharmaceutical field. *Indian J Pharm Educ Res*, **58(3 Suppl)**, s757–s767 (2024) <https://doi.org/10.5530/ijper.58.3s.77>
- [11] Shanmugam B, Srinivasan UM. Formulation and characterization of antibiotic drug loaded aquasome for the topical application. *Future Sci OA*, **10(1)**, FSO949 (2024) <https://doi.org/10.1080/20565623.2024.2367849>
- [12] Ojewumi ME, Ehinmowo AB, Ekanem GP, Nsionu JU, Bolujo EO. Central composite design for solvent extraction of oil from neem (*Azadirachta indica*) seed. *IOP Conf Ser Mater Sci Eng*, **1107(1)**, 012109 (2021) <https://doi.org/10.1088/1757-899X/1107/1/012109>
- [13] Alhamdany AT, Saeed AM, Alaayedi M. Nanoemulsion and solid nanoemulsion for improving oral delivery of a breast cancer drug: formulation, evaluation, and a comparison study. *Saudi Pharm J*, **29(11)**, 1278–1288 (2021) <https://doi.org/10.1016/j.jsps.2021.09.016>
- [14] Wang YW, Jou CH, Yang MC. Effect of quaternized chitosan on the fusion efficiency and cytocompatibility of liposomes. *J Polym Res*, **19(1)**, 9755 (2012) <https://doi.org/10.1007/s10965-011-9755-7>

- [15] Karthik S, Raghavan CV, Marslin G, Rahman H, Selvaraj D, Balakumar K, Franklin G. Quillaja saponin: a prospective emulsifier for the preparation of solid lipid nanoparticles. *Colloids Surf B Biointerfaces*, **147**, 274–280 (2016) <https://doi.org/10.1016/j.colsurfb.2016.07.065>
- [16] Farooq M, Usman F, Zaib S, Shah HS, Jamil QA, Akbar Sheikh F, Khan A, Rabea S, Hagra SA, El-Saber Batiha G, Khan I. Fabrication and evaluation of voriconazole loaded transthesomal gel for enhanced antifungal and antileishmanial activity. *Molecules*, **27(10)**, 3347 (2022) <https://doi.org/10.3390/molecules27103347>
- [17] Das S, Bishal A, Debnath B, Mukherjee S. Advancements in aquasomes-based topical drug delivery for enhanced dermatological treatments. *Dermatol Rev*, **6(1)**, e70014 (2025) <https://doi.org/10.1002/der.7.20014>
- [18] Mourtas S, Fotopoulou S, Duraj S, Sfika V, Tsakiroglou C, Antimisiaris SG. Liposomal drugs dispersed in hydrogels: effect of liposome, drug and gel properties on drug release kinetics. *Colloids Surf B Biointerfaces*, **55(2)**, 212–221 (2007) <https://doi.org/10.1016/j.colsurfb.2006.12.005>
- [19] Aggarwal G, Nagpal M, Kaur G. Development and comparison of nanosponge and niosome based gel for the topical delivery of tazarotene. *Pharm Nanotechnol*, **4(3)**, 213–228 (2016) <https://doi.org/10.2174/2211738504666160804154213>
- [20] Shirsand SB, Para MS, Nagendrakumar D, Kanani KM, Keerthy D. Formulation and evaluation of ketoconazole niosomal gel drug delivery system. *Int J Pharm Investig*, **2(4)**, 201–207 (2012) <https://doi.org/10.4103/2230-973X.107002>
- [21] Harun SN, Nordin SA, Gani SS, Shamsuddin AF, Basri M, Basri HB. Development of nanoemulsion for efficient brain parenteral delivery of cefuroxime: designs, characterizations, and pharmacokinetics. *Int J Nanomedicine*, **13**, 2571–2584 (2018) <https://doi.org/10.2147/IJN.S151788>
- [22] Elangovan S, Arumugam S. Purification, characterization, and biological activities of melanin pigment isolated from Indian squid *Uroteuthis duvaucelii*. *Aquac Int*, **31(6)**, 3095–3108 (2023) <https://doi.org/10.1007/s10499-023-01158-9>
- [23] Miller DP, de Pablo JJ, Corti H. Thermophysical properties of trehalose and its concentrated aqueous solutions. *Pharm Res*, **14(5)**, 578–590 (1997) <https://doi.org/10.1023/A:1012192725996>
- [24] Gupta AK, Gupta D, Gupta V. Aquasomes: a self-assembled nano-particulate carrier system. *Int J Curr Res Rev*, **13(4)**, 44–52 (2021) <https://doi.org/10.31782/IJCRR.2021.13427>
- [25] Bwalya F, Barre L, Erdem M, Kaynak MS. Preparation and characterization of vitamin C aquasomes. *Recent Adv Drug Deliv Formul*, **19(3)**, 290–302 (2025) <https://doi.org/10.2174/0126673878352032250325002719>
- [26] Sayed S, Abdel-Moteleb M, Amin MM, Khowessah OM. Cubogel as potential platform for glaucoma management. *Drug Deliv*, **28(1)**, 293–305 (2021) <https://doi.org/10.1080/10717544.2021.1872740>
- [27] Teo MZ, Loo HL, Goh BH, Chuah LH. Progress in topical nanoformulations against bacterial skin and soft tissue infections—current trends. *Drug Deliv Transl Res*, **15(11)**, 4141–4186 (2025) <https://doi.org/10.1007/s13346-025-01924-7>
- [28] Kulkarni S, Prabhakar B, Shende P. Nanodiamond-based berberine aquasomes for enhancing penetration across epidermis to treat psoriasis. *Int J Pharm*, **656**, 124051 (2024) <https://doi.org/10.1016/j.ijpharm.2024.124051>
- [29] İlhan M, Gültekin HE, Rençber S, Şenyiğit Z, Aydın HH. Aquasomes: a novel platform for drug delivery. In: *Systems of Nanovesicular Drug Delivery*. Academic Press, 191–206 (2022) <https://doi.org/10.1016/B978-0-323-91864-0.00020-6>
- [30] Chrisikou I, Orkoula M, Kontoyannis C. FT-IR/ATR solid film formation: qualitative and quantitative analysis of a piperacillin-tazobactam formulation. *Molecules*, **25(24)**, 6051 (2020) <https://doi.org/10.3390/molecules25246051>
- [31] Toral M, Nova-Ramirez F, Nacaratte F. Simultaneous determination of piperacillin and tazobactam in the pharmaceutical formulation Tazonam® by derivative spectrophotometry. *J Chil Chem Soc*, **57(2)**, 1189–1193 (2012) <https://doi.org/10.4067/S0717-97072012000200028>
- [32] Zakir F, Vaidya B, Goyal AK, Malik B, Vyas SP. Development and characterization of oleic acid vesicles for the topical delivery of fluconazole. *Drug Deliv*, **17(4)**, 238–248 (2010) <https://doi.org/10.3109/10717541003680981>
- [33] Ahmed MM, Fatima F, Anwer MK, Ibnouf EO, Kalam MA, Alshamsan A, Aldawsari MF, Alalaiwe A, Ansari MJ. Formulation and in vitro evaluation of topical nanosponge-based gel containing butenafine for the treatment of fungal skin infection. *Saudi Pharm J*, **29(5)**, 467–477 (2021) <https://doi.org/10.1016/j.jsps.2021.04.010>
- [34] Sakran W, Abdel-Rashid RS, Saleh F, Abdel-Monem R. Ethosomal gel for rectal delivery of domperidone. *Drug Deliv*, **29(1)**, 1477–1491 (2022) <https://doi.org/10.1080/10717544.2022.2072542>
- [35] Budhiraja A, Dhingra G. Development and characterization of a novel antiacne niosomal gel of rosmarinic acid. *Drug Deliv*, **22(6)**, 723–730 (2015) <https://doi.org/10.3109/10717544.2014.903010>
- [36] Damera DP, Kaja S, Janardhanam LS, Alim S, Venuganti VV, Nag A. Synthesis, detailed characterization, and dual drug delivery application of BSA loaded aquasomes. *ACS Appl Bio Mater*, **2(10)**, 4471–4484 (2019) <https://doi.org/10.1021/acsabm.9b00635>
- [37] Shanmugam B, Srinivasan UM. Aquasomes nanoformulation for controlled release of drug and improved effectiveness against bacterial infections. *Ther Deliv*, **15(2)**, 95–107 (2024) <https://doi.org/10.4155/tde-2023-0096>

- [38] Waghule T, Rapalli VK, Singhvi G, Gorantla S, Khosa A, Dubey SK, Saha RN. Design of temozolomide-loaded proliposomes and lipid crystal nanoparticles with industrial feasible approaches: comparative assessment of drug loading, entrapment efficiency, and stability at plasma pH. *J Liposome Res*, **31**(2), 158–168 (2021) <https://doi.org/10.1080/08982104.2020.1748648>
- [39] Vengala P, Dintakurthi S, Subrahmanyam CV. Lactose coated ceramic nanoparticles for oral drug delivery. *J Pharm Res*, **7**(6), 540–545 (2013) <https://doi.org/10.1016/j.jopr.2013.06.015>
- [40] Patel MK, Shah S, Dubey BK, Basedia DK, Jain PK. Formulation and characterization of curcumin-loaded aquasomes for topical fungal treatment. *Asian J Pharm Res Dev*, **13**(1), 10–14 (2025) <https://doi.org/10.22270/ajprd.v13i1.1496>
- [41] Bryson HM, Brogden RN. Piperacillin/tazobactam: a review of its antibacterial activity, pharmacokinetic properties and therapeutic potential. *Drugs*, **47**(3), 506–535 (1994) <https://doi.org/10.2165/00003495-199447030-00008>
- [42] Lee JI, Kim KS, Oh BC, Kim NA, Kim IH, Park CG, Kim SJ. Acute necrotic stomatitis (noma) associated with methicillin-resistant *Staphylococcus aureus* infection in a newly acquired rhesus macaque (*Macaca mulatta*). *J Med Primatol*, **40**(3), 188–193 (2011) <https://doi.org/10.1111/j.1600-0684.2011.00470.x>